Noise-Induced Phase Separation and Time Reversal Symmetry Breaking in Active Field Theories Driven by Persistent Noise

Matteo Paoluzzi,[1,2,*] Demian Levis,[3,4] Andrea Crisanti,[2] and Ignacio Pagonabarraga[3,4]
[1]Istituto per le Applicazioni del Calcolo del Consiglio Nazionale delle Ricerche, Via Pietro Castellino 111, 80131 Naples, Italy
[2]Dipartimento di Fisica, Sapienza Università di Roma Piazzale A. Moro 2, I-00185 Rome, Italy
[3]Departament de Física de la Matèria Condensada, Universitat de Barcelona, C. Martí Franquès 1, 08028 Barcelona, Spain
[4]UBICS University of Barcelona Institute of Complex Systems, Martí i Franquès 1, E08028 Barcelona, Spain

(Received 2 October 2023; revised 23 January 2024; accepted 25 July 2024; published 12 September 2024)

Within the Landau-Ginzburg picture of phase transitions, scalar field theories develop phase separation because of a spontaneous symmetry-breaking mechanism. This picture works in thermodynamics but also in the dynamics of phase separation. Here we show that scalar nonequilibrium field theories undergo phase separation just because of nonequilibrium fluctuations driven by a persistent noise. The mechanism is similar to what happens in motility-induced phase separation where persistent motion introduces an effective attractive force. We observe that noise-induced phase separation occurs in a region of the phase diagram where disordered field configurations would otherwise be stable at equilibrium. Measuring the local entropy production rate to quantify the time-reversal symmetry breaking, we find that such breaking is concentrated on the boundary between the two phases.

DOI: 10.1103/PhysRevLett.133.118301

Introduction—Dynamical field theories provide a powerful framework for investigating collective properties in a variety of systems, ranging from critical phenomena and nonequilibrium phase transitions [1], to the growth of interfaces [2]. Continuum descriptions are also suitable for modeling different materials [3], cell colonies [4], single-cell motion [5], or phase transitions in cell aggregates [6–8]. Focusing our attention on scalar field theories, as in the case of the gas-liquid phase transition, upon introducing nonequilibrium deterministic forces, the so-called model A and model B can be extended to capture the large-scale phenomenology of active systems, e.g., collections of self-propelled agents [9–13]. However, the noise fields, representing the effect of the fast degrees of freedom on the slow ones, are also another source of nonequilibriumness in field theories [14]. In particular, there are no reasons *a priori* to consider delta-correlated stochastic forces, while a natural choice might be rather to consider an exponential decay for the two-point correlation function of the noise [15,16].

In this work, we study nonconserved (model A) and conserved (model B) scalar field theories in $2d$, driven out of equilibrium by time-correlated noise. We document that the nonequilibrium noise is the driver of phase separation in a region of the phase diagram where the corresponding equilibrium system does not display any ordered phase. Because the effect of the persistent noise is to destabilize homogeneous configurations as in the case of self-propulsion in active systems [the so-called motility-induced phase separation (MIPS) [17]], we call this phenomenon noise-induced phase separation (NIPS). However, distinct from the coarse-grained theories of MIPS, NIPS does not require nonequilibrium terms for breaking time-reversal symmetry (TRS) to produce microphase separation [11]. As in the case of MIPS, but without any local nonequilibrium terms in the deterministic force, TRS breaking (TRSB), measured using the entropy production rate, is concentrated at the interface between the two phases.

Correlated noise and active field theories—Models with exponentially correlated noise have been largely employed during the last years in active matter [18–21]. Experiments show that active baths are a source of exponentially correlated noise [22,23]. This picture holds even in dense living materials [24]. Numerical simulations show that the leading order dynamical field theory describing the MIPS critical point is driven by a correlated noise [15]. To provide a concrete example of how the echo of the activity takes the form of a persistent noise on the mesoscopic scale, we consider the practical situation where active particles are in contact with a thermal bath. Even though the effect of thermal diffusion is negligible (for instance, in the case of *E. coli* bacterial baths thermal diffusion is almost 2 orders of magnitude smaller than diffusivity due to activity [22]), once we take into consideration thermal fluctuations, we can coarse grain the dynamics with respect to these fast degrees of freedom, keeping the active force fixed. This is still well justified by experiments: again, in the case of *E. coli*, the relaxation time of thermal degrees of freedom at room temperature is of the order of $\tau_T \sim 10^{-7}$ s while the

*Contact author: matteo.paoluzzi@uniroma1.it

TABLE I. Definitions of F and L for Model A and B.

	$F[\varphi]$	$L(\boldsymbol{x},t)$
Model A	$-(\delta H_{LG}/\delta\varphi)$	$\delta(\boldsymbol{x})K(t)$
Model B	$\nabla^2(\delta H_{LG}/\delta\varphi)$	$-\nabla^2\delta(\boldsymbol{x})K(t)$

persistence time is of the order of $\tau_A \sim 1$ s. This number decreases with bacterial density, but it does not change the orders of magnitude so that we are always in the situation $\tau_A \gg \tau_T$. In the Supplemental Material we report the explicit coarse graining of a model of active Ornstein-Uhlenbeck particles with active and thermal noise showing that the adiabatic average of the thermal fluctuations brings to field theories with correlated noise. In the following, we will explore the implication of this effect on $2d$ scalar field theories.

Model—We consider the relaxation dynamics of a scalar field $\varphi \equiv \varphi(\boldsymbol{x},t)$. φ represents the slow variable we are interested in, as in the case of density fluctuations in the gas-liquid phase transition. The dynamics of φ results from the competition between a deterministic force F and a fluctuating one $\psi \equiv \psi(\boldsymbol{x},t)$. The latter represents the effect of the fast degrees of freedom on φ. Instead of considering the stochastic force as a zero mean and delta correlated noise, we assume ψ to be an annealed variable characterized by a timescale τ which is another control parameter of the model (in the limit $\tau \to 0$, we recover a delta-correlated noise). The dynamics reads

$$\dot{\varphi} = F[\varphi] + \psi \tag{1}$$

with $\langle\psi\rangle = 0$ and $\langle\psi(\boldsymbol{x},t)\psi(\boldsymbol{y},s)\rangle = 2DL(\boldsymbol{x}-\boldsymbol{y},t-s)$, where D sets the strength of the noise and the operator L keeps into account both, a suitable differential operator for describing conserved or nonconserved dynamics, and the time-correlation function of the noise. The expressions for F and L are reported in Table I. We restrict our study to the case where F can be written as the functional derivative of the standard Landau-Ginzburg energy functional

$$H_{\mathrm{LG}}[\varphi] = \int d\boldsymbol{x}\left[\frac{\mu}{2}(\nabla\varphi)^2 + \frac{a}{2}\varphi^2 + \frac{u}{4}\varphi^4\right], \tag{2}$$

so that nonequilibrium is caused solely by the presence of the time-correlated noise ψ. The parameter a sets the distance from the equilibrium critical point $a = 0$ [25].

Phase diagram and NIPS—We start with the mean-field (MF) picture within an effective equilibrium approach. For convenience, we consider the Markovian approximation named unified colored noise (UCN) [30]; it has been shown that the correlated noise shifts the critical point of the Landau model at higher temperatures, i.e., the critical value $a_c(\tau)$ is in general $a_c(\tau) > a$ [31]. Although UCN dynamics does not reproduce the real trajectories [32], it provides useful insight into the stationary properties of the system, especially when the potential generating deterministic forces are characterized by positive curvatures, as in the case of a φ^4 theory approaching the critical point from above. For moving at higher order in τ, we should employ other perturbation schemes [21,33]. In the small-τ regime, one has $H_{\mathrm{eff}} \simeq H_{\mathrm{LG}} + (\tau/2)(H'_{\mathrm{LG}})^2 - \tau H''_{\mathrm{LG}}$, where the prime indicates the derivative with respect to φ. A phase transition to $\varphi \neq 0$ takes place if the configuration $\varphi = 0$ is not stable anymore. We can check the stability of $\varphi = 0$ looking at the second derivative of H_{eff}, given by $H''_{\mathrm{eff}} = H'_{\mathrm{LG}} + \tau[(H''_{\mathrm{LG}})^2 + H'_{\mathrm{LG}}H'''_{\mathrm{LG}}] - \tau H''''_{\mathrm{LG}}$. Since $H''_{\mathrm{eff}}[0] = -3u\tau$, negative for any $\tau > 0$, the system undergoes a phase transition to $\varphi \neq 0$. Since the parameter driving the phase transition is the nonequilibrium noise, we refer to this mechanism as NIPS.

The stationary homogeneous configurations of φ are thus regulated by [26]

$$H_{\mathrm{eff}} = \frac{\tilde{a}}{2}\varphi^2 + \frac{\tilde{u}}{4}\varphi^4 + O(\varphi^6)$$
$$\tilde{a} \equiv a(1+\tau a) - 3u\tau, \qquad \tilde{u} \equiv u(1+4\tau). \tag{3}$$

We obtain that the combination of nonequilibrium noise, parametrized by τ, and nonlinear interactions, whose intensity is tuned by u, renormalizes the coupling constants a and u, i.e., $\tilde{u} \geq u$ so that the nonlinear interaction becomes more important, and $\tilde{a} = \tilde{a}(\tau,u)$, so that it can change its sign. Without nonlinear interactions ($u = 0$), the location of the transition remains untouched at $a = 0$. In the language of quantum field theory, a represents the mass of the scalar field, and thus the mechanism introduced here predicts that, just because of the interaction with the external annealed field ψ of mass $m_\psi = \tau^{-1}$, the field φ can acquire mass whose value is proportional to m_ψ. For $u > 0$, the shift of the critical point (or the mass of the scalar field φ) is given by $\tilde{a} = 0 \equiv a_c(\tau)$, that is

$$a_c(\tau) = \frac{1}{2\tau}\left(\sqrt{1+12u\tau^2} - 1\right). \tag{4}$$

Away from the MF regime (and out from the effective equilibrium), it is not clear how fluctuations and nonequilibrium dynamics change the MF.

We now move to $2d$ using numerical simulations. As in the MF, we observe that the correlated noise drives a phase transition. This is qualitatively shown in Fig. (1) where we report representative configurations of model A [(a),(b)] and B [(c),(d)] away from phase transitions at $\tau = 0$. As one can see, for increasing values of τ, disordered configurations become unstable so that a phase transition takes place. To make quantitative progress, we compute the phase diagram of the model in both cases, model A and model B. The result is shown in Fig. 1(e). We observe that by tuning τ the system undergoes a nonequilibrium phase

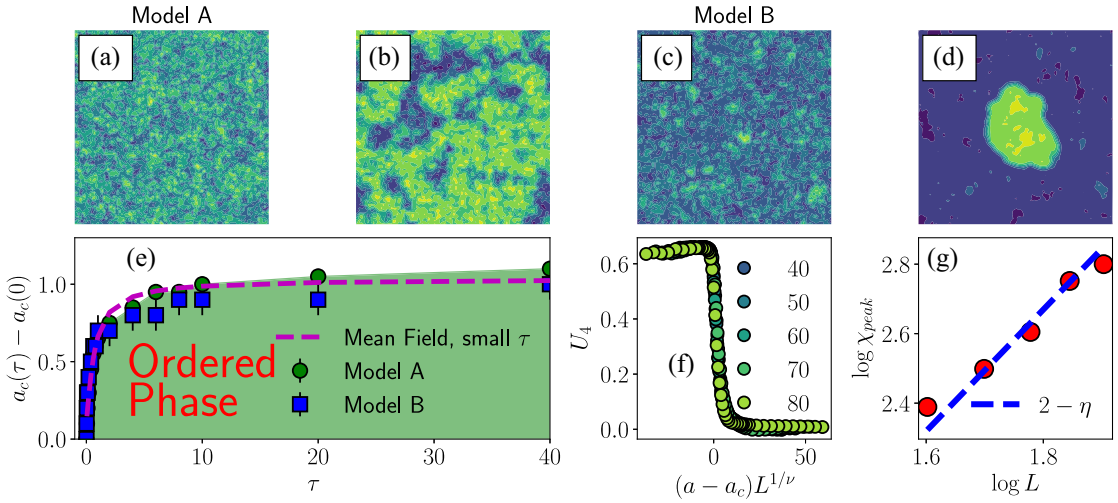

FIG. 1. Noise-induced phase separation (NIPS). (a)–(d) Stationary configurations of model A [(a),(b)] and model B [(c),(d)] in a region of the phase diagram where the equilibrium dynamics leads to a disordered phase [$a(\tau) - a(0) > 0$]. Upon increasing τ (model A: $\tau = 0.02$, 2, model B: $\tau = 0.05$, 10, from left to right), model A orders and model B develops phase separation. The lattice size is $L = 100$ ($D = 1$). (e) Phase diagram for model A and B. The green region indicates where the probability distribution function $\mathcal{P}[\varphi]$ is double peaked. The dashed magenta line is the one parameter fit to Eq. (4). (f) Rescaled Binder parameter for $\tau = 1$ with $\nu = 1$ and different system sizes from $L = 40$ to $L = 80$ (see legend). (g) Scaling of the susceptibility for $\tau = 1$ is consistent with $\eta = 1/4$.

transition in a wide region of the phase diagram where the corresponding equilibrium system is homogeneous. We compare the numerical results with the theoretical prediction (4) using u as a fitting parameter [this is because u in (4) is the MF value and not the one renormalized by fluctuations]. As one can see, the theory reproduces remarkably well the order-disorder transition in a wide range of τ (with $u_{\rm fit} \simeq 0.1$). This is counterintuitive since Eq. (4) has been obtained within the small-τ limit. We can rationalize this by noticing that φ in the Landau theory of continuous transition is arbitrarily small at the transition so that the correction to the mass $\tau H''_{\rm LG} \simeq \tau u \varphi^2$ around the critical point is small in a wide range of τ.

To provide an estimate of the critical exponent ν of model A, we now compute the Binder parameter $U_4 \equiv 1 - \langle \varphi^4 \rangle / 3 \langle \varphi^2 \rangle^2$ for system sizes $L = 40$, 50, 60, 70, 80, and $\tau = 1$ (see [26] for details). As shown in Fig. 1(f), we observe a good scaling collapse within the Ising universality class, i.e., $\nu = 1$. Measuring the exponent η through the scaling of the peak of the susceptibility χ, we observe again a value consistent with the Ising universality class [Fig. 1(g)].

Next, we measure how nonequilibrium fluctuations modify the phase separation region in model B. We thus performed numerical simulations for $\tau = 0.1$, 1, 10, 40 and several values of the initial density $\varphi_a \equiv \int d\boldsymbol{x}\, \varphi(\boldsymbol{x}, 0)$. Figure (2) reports the phase-separation region as τ increases. We observe that not only τ is the trigger for the phase separation, but it also quantitatively impacts the size of the phase-separated region making it larger and larger for increasing values of τ (the scaling of the size of the phase separation region with τ is shown in [26]).

TRSB—As NIPS is driven by nonequilibrium fluctuations, a natural question is whether the noise is just a trigger for an equilibriumlike transition. To answer this question we look at the total entropy production rate $\mathcal{S}$. $\mathcal{S}$ has been the subject of intense studies during the last decades for rationalizing the thermodynamics of active matter [34–37]. For our purpose, $\mathcal{S}$ is a proxy for measuring the breakdown of time reversal symmetry [36,37]. $\mathcal{S}$ is defined as the long-time behavior of Kullback-Leibler divergence [38]

$$\mathcal{S} \equiv \lim_{T\to\infty} \frac{1}{T} \left\langle \log \frac{P[\varphi]}{P_R[\varphi]} \right\rangle \tag{5}$$

with $P[\varphi]$ indicating the probability of the path $\varphi(\boldsymbol{x}, t)$ with $t \in [t_0, T]$ and $P_R[\varphi]$ the probability of the time-reversed

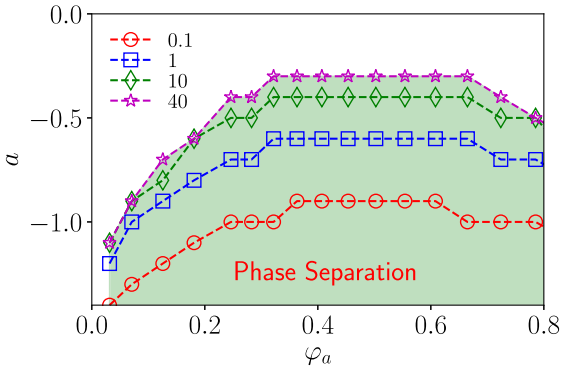

FIG. 2. Nonequilibrium dynamics enhances phase separation. Phase diagrams of model B for different values of τ (see legend). The green area indicates the phase separation region (corresponding to $\tau = 40$) that increases monotonically for increasing values of τ (see [26]).

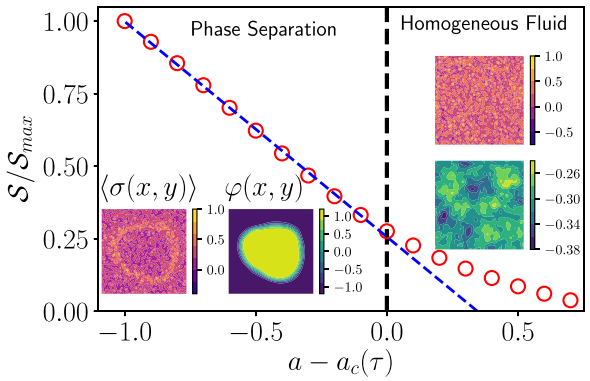

FIG. 3. Entropy production rate and phase separation. Total entropy production rate $\mathcal{S}$ as a function of the distance from the transition point, i.e., $a_c(\tau) - a$, in the case of model B ($\tau = 1$). $\mathcal{S}$ linearly increases in the phase-separated regime (see the blue dashed line as a guide to the eye). Insets: representative stationary configuration of the conserved field φ and the corresponding local entropy production rate σ.

path φ_R obtained through the transformation $t \to T - t$. In the case of a field theory, $\mathcal{S}$ can be written in terms of a spatial resolved entropy production rate $\sigma(\boldsymbol{x})$ so that $\mathcal{S} = \int d\boldsymbol{x}\, \sigma(\boldsymbol{x})$ where $\sigma(\boldsymbol{x})$ is a model-dependent composite operator of the field φ [11,16,39]. In the case of model B, the computation of $\mathcal{S}$ brings us to [26]

$$\sigma(\boldsymbol{x}) = \frac{\tau^2}{2D}\left\langle \dot{\varphi}^3 \frac{\delta^3 H_{\mathrm{LG}}}{\delta \varphi^3} \right\rangle \tag{6}$$

where the angular brackets indicate the averaging over time performed on a stationary configuration (the presence of the cutoff $\Lambda = 2\pi/\ell$, with ℓ the lattice spacing, avoids any ultraviolet divergence). We highlight that the expression we arrive at is the same obtained earlier for model A [16] and in the case of active Ornstein-Uhlenbeck particles [21,33].

We employ (6) for computing $\mathcal{S}$ in simulations. Figure 3(a) reports $\mathcal{S}$ ($\tau = 1$). As an initial condition, we consider a drop of radius $R = 20$ ($L = 60$). We observe that $\mathcal{S}$ increases approaching the transition. As in other nonequilibrium field theories [40,41], $\mathcal{S}$ undergoes a crossover at the transition where it starts to grow linearly for a decreasing value of a. Because $\mathcal{S}$ is nonzero, despite the phase separation being equilibriumlike, TRS remains broken.

Another natural question is whether TRSB is accompanied by some nonequilibrium pattern formation. We thus look at the map $\sigma(\boldsymbol{x})$. In Fig. (3) we display the field configurations and the corresponding $\sigma(\boldsymbol{x})$ (see the insets). In the symmetric phase, φ is disordered in space and the same happens for σ. Once the system phase separates, the corresponding map of σ develops a pattern at the boundary between the two phases, indicating that most TRSB is concentrated in that region. This is precisely the kind of pattern observed in experiments and simulations of active systems in a model-independent fashion [42]. We can

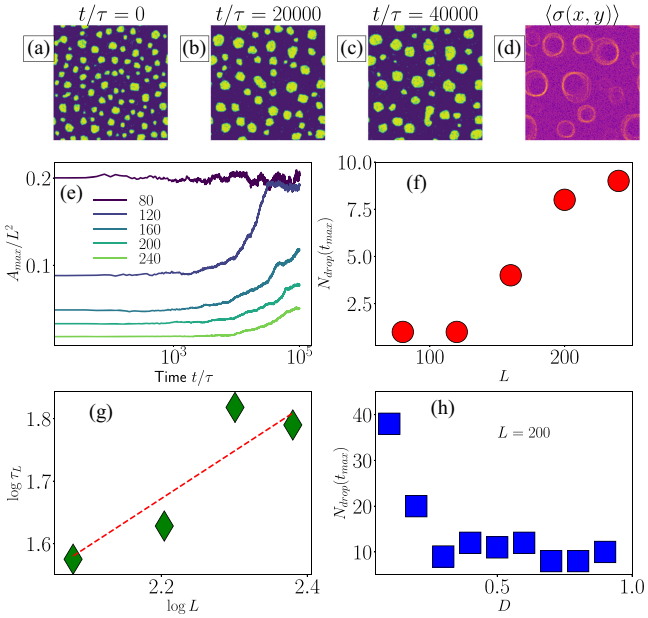

FIG. 4. Microphase separation. (a)–(c) Phase-separated configurations ($\tau = 0.5$, $a = -3$) for the larger system size $L = 240$ at different times. (d) Entropy production rate field. (e) Drop area as a function of time for different system sizes (see legend). (f) Number of drops in the final configuration as a function of the system sizes. (g) Relaxation time τ_L of microphase as a function of the system size L (the dashed line power law scaling is a guide to the eye). (h) Number of drops as a function of the noise strength D.

rationalize that from (6), noticing that terms proportional to $\varphi^m \nabla^2 \varphi$, with $m > 1$, that give a contribution to σ on the boundary between the two phases, arise once we replace $\dot{\varphi}$ by Eq. (1), so that $\sigma \sim \langle(\mu\nabla^2\varphi - a\varphi + u\varphi^3 + \psi)^3\varphi\rangle$. These terms are irrelevant in the renormalization group sense [16], however, similarly to the case of active model B (but distinct since we do not have any nonequilibrium gradient term in F), they contribute to a space-dependent TRSB. In the case of model A, the order parameter is not conserved and thus interfaces are suppressed in favor of homogeneous phases that spontaneously break the $\varphi \to -\varphi$ symmetry. σ might develop anomalous fluctuations around the upper critical dimensions $d_c = 4$ [12,16], which is far away from our numerical study.

Microphase separation and coarsening—The nonequilibrium noise impacts the morphology of the phase separation: we observe that, deep in the phase-separated region, model B develops microphases [43,44], as shown in Figs. 4(a)–4(c) ($L = 240$, $a = -3$, and $\tau = 0.5$) where we report typical configurations at different times for $L = 240$ [26]. In Fig. 4(d) we show σ that signal TRSB along the edge of each drop. Performing longer simulations ($N_t = 1.2 \times 10^7$ steps) for several system sizes ranging from $L = 80$ up to $L = 240$ we document a crossover from microphase separation to coarsening. Figure 4(e) shows how the area covered by the larger drop $A_{\max}$ evolves for

different system sizes (we wait 2×10^6 steps before collecting data, $\tau = 0.5$ and $a = -3$). The time spent in configurations with small drops, i.e., the larger drop does not exceed the 10% of the box area, increases with L. In other words, after developing microphases, the system undergoes a coarsening dynamics towards a single large droplet after decreasing the system sizes. In the thermodynamic limit, the system never reaches the coarsening regime but remains microphase separated. This is documented also in Fig. 4(f) where we report the number of drops in the final configuration. We thus measure the characteristic lifetime τ_L of the microphase by fitting to an exponential decay the number of drops $N_{\text{drops}}(t)$ as a function of time. The result of this analysis is reported in Fig. 4(g) for different system sizes L. We obtain that τ_L increases linearly with L. Finally, we explore the effect of the strength of the noise D [see Fig. 4(h)]. We obtain that the number of drops increases significantly as D decreases, as in the case of active model B+ [45].

Discussion—We have shown that scalar field theories in the MF and $2d$ undergo a phase transition driven by nonequilibrium noise and controlled by its persistence time τ. The phase separation occurs in a region of the phase diagram where the corresponding equilibrium model is homogeneous. We showed that the emerging phenomenology can be rationalized within a simple MF theory within the small-τ limit. The theory highlights how the combination of nonlinearities (parametrized by u) and nonequilibrium noise (parametrized by τ) can trigger the transition. We computed numerically the critical exponents that are compatible with the Ising universality class [46]. The numerical computation of $\mathcal{S}$ indicates that NIPS breaks TRS making the phase separation distinct from that of the equilibrium model. Again, TRSB is due to the combination of nonlinear interactions and nonequilibrium dynamics: both ingredients are fundamental and complementary. In other words, even though the critical point belongs to the Ising universality class, phase separation is maintained because of the continuous energy injection on the mesoscopic scale due to the noise. Because of that, $\mathcal{S} \neq 0$ for any arbitrary small value of τ. Finally, we observed that most of the TRSB is concentrated at the boundaries between the two coexisting phases. It is worth noting that the picture we obtain is quite similar to that of active model B. On the other hand, in our model, TRSB is caused by the presence of nonequilibrium fluctuations that couple with each other because of nonlinear interactions. We also documented other features of scalar active matter that usually require extra nonequilibrium terms in the framework of active model B, such as microphase separation [45,47–49].

Finally, we observe that time-correlated noise naturally emerges in the continuum description of active matter. For instance, the set of continuum equations usually takes the form $\partial_t \rho = -\nabla[J - D(\rho)\nabla\rho]$ with a current J decaying on a finite timescale, i.e., $\partial_t J = -D_r J + \cdots$ [9,50–52]. To perform the linear stability analysis one considers J as a fast variable so that it can be removed adiabatically $\dot{J} = 0$. If we remove this assumption, ∇J acts as an Ornstein-Uhlenbeck field on ρ. Our results suggest that, once we include nonlinear interactions, the Ornstein-Uhlenbeck field destabilizes homogenous profiles, even in the small (but not vanishing) τ regime.

Acknowledgments—M. P. acknowledges NextGeneration EU (CUP B63C22000730005), Project IR0000029—Humanities and Cultural Heritage Italian Open Science Cloud (H2IOSC)—M4, C2, Action 3.1.1. D. L. acknowledges DURSI and AEI/MCIU for financial support under Projects No. 2021SGR00673 and No. PID2022-140407NB-C22. I. P. acknowledges support from MICINN and DURSI for financial support under Projects No. PID2021-126570NB-100 AEI/FEDER-EU and No. 2021SGR-673, respectively, and from Generalitat de Catalunya under Program Icrea Acadèmia.

[1] U. C. Täuber, *Critical Dynamics: A Field Theory Approach to Equilibrium and Non-Equilibrium Scaling Behavior* (Cambridge University Press, Cambridge, England, 2014).
[2] M. Kardar, G. Parisi, and Y.-C. Zhang, Phys. Rev. Lett. **56**, 889 (1986).
[3] V. M. Kendon, M. E. Cates, I. Pagonabarraga, J.-C. Desplat, and P. Bladon, J. Fluid Mech. **440**, 147 (2001).
[4] M. E. Cates, D. Marenduzzo, I. Pagonabarraga, and J. Tailleur, Proc. Natl. Acad. Sci. U.S.A. **107**, 11715 (2010).
[5] E. Tjhung, D. Marenduzzo, and M. E. Cates, Proc. Natl. Acad. Sci. U.S.A. **109**, 12381 (2012).
[6] F. Ziebert, S. Swaminathan, and I. S. Aranson, J. R. Soc. Interface **9**, 1084 (2012).
[7] B. Loewe, M. Chiang, D. Marenduzzo, and M. C. Marchetti, Phys. Rev. Lett. **125**, 038003 (2020).
[8] D. Wenzel and A. Voigt, Phys. Rev. E **104**, 054410 (2021).
[9] M. C. Marchetti, J. F. Joanny, S. Ramaswamy, T. B. Liverpool, J. Prost, M. Rao, and R. A. Simha, Rev. Mod. Phys. **85**, 1143 (2013).
[10] R. Wittkowski, A. Tiribocchi, J. Stenhammar, R. J. Allen, D. Marenduzzo, and M. E. Cates, Nat. Commun. **5**, 4351 (2014).
[11] C. Nardini, É. Fodor, E. Tjhung, F. Van Wijland, J. Tailleur, and M. E. Cates, Phys. Rev. X **7**, 021007 (2017).
[12] F. Caballero and M. E. Cates, Phys. Rev. Lett. **124**, 240604 (2020).
[13] M. E. Cates, Rep. Prog. Phys. **75**, 042601 (2012).
[14] J. Sancho, J. Garcia-Ojalvo, and H. Guo, Physica (Amsterdam) **113D**, 331 (1998).
[15] C. Maggi, N. Gnan, M. Paoluzzi, E. Zaccarelli, and A. Crisanti, Commun. Phys. **5**, 1 (2022).
[16] M. Paoluzzi, Phys. Rev. E **105**, 044139 (2022).
[17] J. Tailleur and M. E. Cates, Phys. Rev. Lett. **100**, 218103 (2008).
[18] G. Szamel, Phys. Rev. E **90**, 012111 (2014).
[19] C. Maggi, U. M. B. Marconi, N. Gnan, and R. Di Leonardo, Sci. Rep. **5**, 10742 (2015).

[20] T. F. F. Farage, P. Krinninger, and J. M. Brader, Phys. Rev. E **91**, 042310 (2015).
[21] E. Fodor, C. Nardini, M. E. Cates, J. Tailleur, P. Visco, and F. van Wijland, Phys. Rev. Lett. **117**, 038103 (2016).
[22] C. Maggi, M. Paoluzzi, N. Pellicciotta, A. Lepore, L. Angelani, and R. Di Leonardo, Phys. Rev. Lett. **113**, 238303 (2014).
[23] C. Maggi, M. Paoluzzi, L. Angelani, and R. Di Leonardo, Sci. Rep. **7**, 17588 (2017).
[24] S. Henkes, K. Kostanjevec, J. M. Collinson, R. Sknepnek, and E. Bertin, Nat. Commun. **11**, 1 (2020).
[25] Below the upper critical dimension, this critical value will be renormalized to lower values because fluctuations are not negligible.
[26] See Supplemental Material at http://link.aps.org/supplemental/10.1103/PhysRevLett.133.118301, which contains additional details on the model, additional results complementing those shown in the main text, and includes Refs. [27–29].
[27] D. J. Amit and V. Martin-Mayor, *Field Theory, the Renormalization Group, and Critical Phenomena: Graphs to Computers* (World Scientific Publishing Company, Singapore, 2005).
[28] K. Binder, Z. Phys. B Condens. Matter **43**, 119 (1981).
[29] D. S. Dean, J. Phys. A **29**, L613 (1996).
[30] P. Hänggi and P. Jung, Adv. Chem. Phys. **89**, 239 (1995).
[31] M. Paoluzzi, C. Maggi, U. Marini Bettolo Marconi, and N. Gnan, Phys. Rev. E **94**, 052602 (2016).
[32] A. Crisanti and M. Paoluzzi, Phys. Rev. E **107**, 034110 (2023).
[33] D. Martin, J. O'Byrne, M. E. Cates, E. Fodor, C. Nardini, J. Tailleur, and F. van Wijland, Phys. Rev. E **103**, 032607 (2021).
[34] R. Bebon, J. F. Robinson, and T. Speck, arXiv:2401.02252.
[35] É. Fodor, R. L. Jack, and M. E. Cates, Annu. Rev. Condens. Matter Phys. **13**, 215 (2022).
[36] T. Markovich, E. Fodor, E. Tjhung, and M. E. Cates, Phys. Rev. X **11**, 021057 (2021).
[37] Ø. L. Borthne, É. Fodor, and M. E. Cates, New J. Phys. **22**, 123012 (2020).
[38] J. L. Lebowitz and H. Spohn, J. Stat. Phys. **95**, 333 (1999).
[39] G. Pruessner and R. Garcia-Millan, arXiv:2211.11906.
[40] H. Alston, L. Cocconi, and T. Bertrand, Phys. Rev. Lett. **131**, 258301 (2023).
[41] T. Suchanek, K. Kroy, and S. A. M. Loos, Phys. Rev. Lett. **131**, 258302 (2023).
[42] S. Ro, B. Guo, A. Shih, T. V. Phan, R. H. Austin, D. Levine, P. M. Chaikin, and S. Martiniani, Phys. Rev. Lett. **129**, 220601 (2022).
[43] J. Stenhammar, D. Marenduzzo, R. J. Allen, and M. E. Cates, Soft Matter **10**, 1489 (2014).
[44] C. B. Caporusso, P. Digregorio, D. Levis, L. F. Cugliandolo, and G. Gonnella, Phys. Rev. Lett. **125**, 178004 (2020).
[45] E. Tjhung, C. Nardini, and M. E. Cates, Phys. Rev. X **8**, 031080 (2018).
[46] The accurate numerical computation of the critical exponents requires separate work.
[47] F. Caballero, C. Nardini, and M. E. Cates, J. Stat. Mech. (2018) 123208.
[48] G. Fausti, E. Tjhung, M. E. Cates, and C. Nardini, Phys. Rev. Lett. **127**, 068001 (2021).
[49] X.-q. Shi, G. Fausti, H. Chaté, C. Nardini, and A. Solon, Phys. Rev. Lett. **125**, 168001 (2020).
[50] T. Speck, A. M. Menzel, J. Bialké, and H. Löwen, J. Chem. Phys. **142**, 224109 (2015).
[51] Y. Fily and M. C. Marchetti, Phys. Rev. Lett. **108**, 235702 (2012).
[52] U. M. B. Marconi, L. Caprini, and A. Puglisi, New J. Phys. **23**, 103024 (2021).